BNWL-SA- 1107

0/0
1
8/14/70

EXPERIMENTS AND CALCULATIONS FOR H_2O-MODERATED ASSEMBLIES CONTAINING UO_2-2 wt.% PuO_2 FUEL RODS [a]

By

V. O. Uotinen [b]
L. D. Williams [c]

Battelle Memorial Institute
Pacific Northwest Laboratory
Richland, Washington

May 23, 1967
~~February 10, 1967~~

Paper for oral presentation and publication in the proceedings of the Thirteenth Annual American Nuclear Society Meeting, San Diego, California, June 11-15, 1967.

(a) This paper is based on work performed under United States Atomic Energy Commission Contract AT(45-1)-1830.

(b) Research Scientist, Nuclear Experiments and Analyses Section, and
(c) Development Engineer, Heavy Moderator Reactor Physics,
Reactor Physics Department, Pacific Northwest Laboratory,
Operated by Battelle Memorial Institute for the United States Atomic Energy Commission, Richland, Washington.

P6276

DISCLAIMER

EXPERIMENTS AND CALCULATIONS FOR H_2O-MODERATED ASSEMBLIES CONTAINING UO_2- 2 wt.% PuO_2 FUEL RODS

V. O. Uotinen, L. D. Williams

INTRODUCTION

Critical experiments have been performed in the Plutonium Recycle Critical Facility[1] (PRCF) in six configurations of UO_2-2 wt% PuO_2 fuel rods. Each rod is made of 1128 g of UO_2-PuO_2 and is 36 in. long, 0.508 in. in diameter, and clad with 0.030 in. of Zircaloy-2. The rods are of three types which have respectively the following weight percent of $^{239}Pu/^{240}Pu/^{241}Pu/^{242}Pu$:

1) 91.62/7.65/0.70/0.03

2) 81.11/16.54/2.15/0.20

3) 71.76/23.50/4.08/0.66

The rods were in a hexagonal lattice with a lattice spacing of 0.85 in. and a water-to-oxide volume ratio of 1.83.

Single-zone cores were studied using fuel types 1 and 3. Two-zone cores were studied using various combinations of the three fuel types. An effectively infinite H_2O reflector surrounded the core.

Measured parameters that are summarized here include critical mass; spatial flux and power distributions; power peaking and power sharing; bucklings, reflector savings; worth of fuel rods; moderator void worth; moderator level reactivity coefficient; moderator temperature reactivity coefficient; and the ratio of effective delayed-neutron fraction to mean neutron lifetime, β/ℓ. Measurements of reactivity worth of absorbing rods have been reported earlier.[2]

Calculations have been performed using the same methods that have been used in analyses of other plutonium-fueled, H_2O moderated experiments.[3,4,5] They consist of using the codes HRG,[6] THERMOS,[7] and TEMPEST[8] to obtain four energy-group, cell-averaged cross sections, and HFN[9] to calculate multiplications and spatial distributions of power and flux.

II. SUMMARY

This paper presents a summary of the experimental results and preliminary analytical correlations. A comparison is made between two methods of measuring buckling.

The calculational results that are presented constitute a preliminary evaluation of the standard calculational scheme that is used at BNW for reactor physics design calculations. Previously this scheme has been evaluated for its ability to predict critical masses and multiplications.[4,5] We are currently evaluating its ability to predict other properties of Pu-fueled, H_2O-moderated cores. The work reported here is a step in this direction.

In many cases the preliminary calculational techniques need to be refined. The techniques for analyzing each individual experiment are being developed, and more detailed analyses will be reported later.

III. DESCRIPTION OF LATTICE

The fuel rods rested on a lucite plate 3/4 in. thick and were positioned in an equilateral triangular lattice (0.85 in. spacing) by two lucite lattice plates 3/4 in. thick. Some of the holes in the lattice were slightly over-sized, and fuel rods that occupied such positions were enclosed in lucite sleeves.

Three cadmium safety sheets were situated in the reflector symmetrically surrounding the core. When the safety sheets were withdrawn they were replaced by lucite followers. Three control elements were also provided. Each control "element" consisted of a cluster of four Cd rods which moved as a unit; when the control rods were removed they were replaced by fuel follower rods which were always of fuel type 1 (See Introduction).

IV. CALCULATIONAL METHODS

Calculations have been performed using methods that have been used previously in analyses of other plutonium-fueled, H_2O moderated experiments.[3,4,5] They consist of using the codes HRG,[6] THERMOS,[7] and TEMPEST[8] to generate four energy-group cross sections, and HFN[9] to calculate the effective leakage from the finite assembly and obtain multiplication and spatial distributions of power and flux. The boundaries of the energy groups are defined in Table I.

The unit lattice cell was assumed to consist of three regions: 1) fuel, 2) cladding, and 3) moderator. Reflecting cell boundary conditions were assumed, and no additional heavy scatterer region was assumed.

Cell-averaged macroscopic thermal cross sections were computed using the codes THERMOS and TEMPEST. TEMPEST was used in computing only the thermal diffusion coefficient, defined as $1/(3\bar{\Sigma}_{tr})$. For the TEMPEST calculation the cell density of each isotope was weighted by a flux depression factor (ratio of average flux in region to average flux in cell) obtained from the THERMOS calculation.

Gas model scattering kernels were used for all materials except hydrogen. The Nelkin[10] kernel with an approximate correction[11] for anisotropic scattering was used for hydrogen, except in the analysis of the temperature coefficient experiments, in which case isotropic scattering was assumed.

Macroscopic cross sections for the three non-thermal groups were computed with the HRG code. The B_1 approximation was used with the ^{239}Pu fission spectrum. Resonance absorption was calculated for the isotopes ^{239}Pu, ^{240}Pu, and ^{238}U. The effect of surrounding rods in the lattice was corrected for with Dancoff-Ginsburg correction factors obtained from published tables.[12]

Thermal constants for the H_2O reflector were obtained from a calculation using the TEMPEST code, assuming the Wigner-Wilkins spectrum. Non-thermal constants were obtained from an HRG calculation in which the P_1 approximation and the ^{239}Pu fission spectrum were assumed.

All microscopic cross sections were obtained from the BNW Master Library.[13] The thermal cross sections for ^{235}U, ^{239}Pu and ^{241}Pu are normalized to those of the Westcott evaluation.[14]

V. CRITICAL MASS

The critical mass with full moderator height and with all control elements completely withdrawn, was determined for each of the loadings. Measurements were then made to determine the reactivity worth of lucite templates, sleeves, and safety sheet followers, and of the control rod fuel follower rods. These results were used to correct the measured critical mass for these perturbations. The resulting corrected critical number of fuel rods represents a "clean" loading. The critical mass measurements are summarized in Table II. The second column from the right in Table II is the "clean" critical number of fuel rods; it includes corrections for the various perturbations that were present in the PRCF.

In the last column of Table II are listed the calculated effective multiplications, which are from one-dimensional, radial calculations using the diffusion theory code HFN. The radii used in the calculations correspond to the effective radii of the measured clean critical loadings.

VI. SPATIAL ACTIVATION DISTRIBUTIONS

Spatial distributions of copper pin activity were measured in the axial and radial directions in the two single-zone cores, and in the radial direction in all two-zone cores.

Typical radial distributions of sub-cadmium activity are shown in Figures 1 and 2, for a single-zone and a two-zone core, respectively. Also shown in the Figures are thermal activation distributions that were calculated with the code HFN. The thermal activation cross sections used in the various zones are cell-averaged values. The core radius was the effective cylindrical radius based on the actual number of fuel rods present during the experiment. Calculated and measured distributions were normalized using normalization factors that were averaged for the positions two, three, and four lattice units from the center.

The agreement between calculation and experiment is considered good except near the core-reflector boundary and near the center of the core. The disagreement at the center is due to a flux depression which was measured at the center of each core. The disagreement in the boundary region between core and reflector is probably due to neglecting the changing spectrum in this region. Attempts are being made to obtain better agreement in this region by taking into account the changes in spectrum near the boundary.

VII. POWER DENSITY DISTRIBUTIONS

Spatial distributions of relative power density were obtained by measuring the gamma-ray activities of fuel rods after short irradiations ($\sim$ 1 hr.) at low power levels ($\sim$ 100 w). Axial and radial distributions were measured in five of the six cores. The radial distributions in the two-zoned cores provide a measurement of power sharing between different types of fuels.

Typical distributions of power density in the radial direction are shown in Figures 3 and 4 for a single-zone and a two-zone core, respectively. Also shown are curves calculated with the HFN code. The core radius was

the effective cylindrical radius based on the number of fuel rods present during the experiment. Each experimental point represents the average power density over the thickness of a fuel rod, and is plotted at the effective cylinderized radius for the fuel rod. The calculated curves were normalized to an average power density of unity; the measured points were normalized to the calculated curve using average normalization factors as explained in the preceding section.

As in the case of activation distributions, the agreement between calculation and experiment is reasonably good, except near the core-reflector boundary and at the center of the core. Calculated and measured power sharing factors in zoned cores (ratio of power density in a fuel rod to power density in a fuel rod of the other type at the same radius) agree in all cases to within 2%.

Power Peaking. Radial distributions of relative power density were measured in the two single-zone cores with a water hole in the center; the water hole was formed by removing the central fuel rod. Calculated local-to-average power peaking factors in rods adjacent to the water hole are greater than measured values by $\sim$ 5-6%. However, calculated ratios of (av. power in rod adjacent to H_2O hole)/(av. power in same rod with no H_2O hole present) agree with measured values to better than 1%.

VIII. BUCKLING AND REFLECTOR SAVINGS

Radial and axial bucklings and reflector savings were deduced from two types of measurements, 1) spatial distribution of thermal activation of copper pins, and 2) spatial distribution of gamma-ray activity from fuel rods. Functions of the form

$$y = A_1 \cos[A_2(X-A_3)] \qquad (1)$$

were fitted to axial distributions, and functions of the form

$$y = A_1 J_o\left[\left(\frac{X-A_2}{A_3}\right) 2.405\right] \qquad (2)$$

were fitted to radial distributions. The J_o is the Bessel function of the first kind of order zero. In Equation (1) A_2 is the square root of the axial buckling. In Equation (2) A_3 is the effective radius of the core, and is related to the radial buckling B_r^2 by the equation

$$B_r^2 = \left(\frac{2.405}{A_3}\right)^2 . \qquad (3)$$

In all cases data points that were near the core-reflector boundary were not included when making the fits. Several fits were made, using fewer points in each successive fit. The fit that resulted in the smallest standard deviation in the buckling was chosen as the "best" fit. In the case of axial gamma-scans, several rods, located at different radii in the core, were scanned. No systematic variation was noted in axial buckling as a function of radius. This was true for both the uniform and zoned loadings.

The axial reflector savings is defined as the difference between the effective height, determined from the best fit, and the height of the fuel, 36 in. The radial reflector savings is defined as the difference between the effective radius, determined from the best fit, and the "actual" radius, which is defined as

$$R = \sqrt{\frac{NA}{\pi}} , \qquad (4)$$

where N is the number of fuel rods in the core, and A is the area of a unit cell.

Calculated bucklings and reflector savings were obtained by fitting functions of the form of Equations (1) and (2) to calculated distributions of power density and thermal flux. Measured and calculated results are compared in Table III.

Comparison of Experimental Methods. The reflector savings measured in these experiments allow a comparison to be made between the results of a critical "flux shape" method and a subcritical method.[3, 15] The subcritical method combines a critical mass measurement (extrapolation from multiplication measurements) with an exponential experiment, to obtain a value for the reflector savings assuming the axial and radial reflector savings are equal. The material buckling as determined from the exponential measurements is equated to the critical geometric buckling as determined from the approach-to-critical experiment. This results in the equation

$$B^2 = \left(\frac{2.405}{R_{\text{crit.size}} + \lambda}\right)^2 + \left(\frac{\pi}{H+2\lambda}\right)^2 = \left(\frac{2.405}{R_{\text{expon.}} + \lambda}\right)^2 - \gamma_{11}^2 \qquad (5)$$

where λ is the reflector savings and $-\gamma_{11}$ is the slope of the plot of natural logarithm of flux against axial position. One other assumption that is evident in Equation (5) is that the radial reflector savings of the exponential loading is assumed to be equal to that of the critical loading.

The reflector savings that is obtained by solving Equation (5) represents an "average" value of the reflector savings. The error that is introduced by using this "average" reflector savings to determine critical bucklings is small if the radius of the core is nearly the same magnitude as the height of the fuel, for then the axial and radial reflector savings are expected to be equal. However, the error is not negligible if the radius is small with respect to the height, for in this case the reflector savings in the radial and axial directions are expected to be different.

Results of subcritical experiments using UO_2-2 wt.% PuO_2 fuel rods have been reported.[3] Although a subcritical experiment was not performed at a lattice spacing of 0.85 in., we can estimate the reflector savings for a 0.85 in. lattice by interpolating between the results presented in Reference 3. A comparison is presented in Table IV between reflector savings, bucklings, and critical number of rods determined using the subcritical and critical methods. The bucklings and critical number of rods were obtained from analytical functions that were fitted[16] to the measurements reported in Reference 3. The subcritical method results in reasonable "average" reflector savings. Bucklings determined by the two methods disagree by 1% for the larger core and by 6% for the smaller core. One should remember that the accuracy of the flux shape method also decreases as the core radius decreases; this is because in a small core there are only a few lattice positions available for measurements to be made. Thus, the only conclusion that is made is that bucklings determined by these two methods show reasonable agreement in the case of the larger core, but disagree significantly in the case of the smaller core.

While making this conclusion we must bear in mind that the subcritical results used in this comparison were not actually measured at this lattice pitch, but were obtained by interpolating between measured results at other lattice pitches.

In any event, this comparison illustrates the difficulties inherent in the measurement of bucklings for small cores and in the interpretation of bucklings measured by various techniques. As has been pointed out recently,[17] there is a need for further work in this area to clarify the differences between various techniques for measuring bucklings.

IX. FUEL ROD WORTH

The worth of a fuel rod replacing water was measured as a function of radius in the two single-zone cores. The results are plotted in Figure 5.

The difference in k_{eff} when a fuel rod replaces water in the center and at the periphery of the core was calculated with the code HFN. Calculated worths of fuel rods in the center and on the periphery of the reactor are compared with measured worths in Table V.

Calculated fuel rod worths depend on what lattice constants are chosen to represent water. In our case, the constants were those for an infinite water medium. Better agreement with experimental results would be expected if one would take into account the changes in spectrum near core-water boundaries.

X. MODERATOR VOIDING

Worths of cylindrical (tube) voids and annular (film) voids were measured as a function of radius in the two single-zone cores. The tube void was formed by a lucite tube with an I.D. of 0.625 in. The annular film void replaced a 14% of the moderator in a cell around a fuel rod; this void was formed by a lucite tube (0.625 in. I.D.) which surrounded the fuel rod. The annular region between fuel rod and lucite thimble was filled with either water or air; and the difference in reactivity between these two cases was taken to be the worth of the void. The results are plotted in Figure 6.

By summing the worths of individual film voids one can obtain an estimate of the worth of simultaneously voiding the entire moderator by 14%. Such a value is an estimate because it does not take into account interactions among cells, and because the exact shape of the curve is not known.

Calculations were performed of the change in k_{eff} produced by a 14% void in the central cell, and by a 14% voiding of the entire moderator. Measured and calculated results are summarized in Table VI.

XI. MODERATOR LEVEL REACTIVITY COEFFICIENT

Moderator level reactivity coefficients were measured in five of the six cores. In some cases measurements were made in the top reflector only; in other cases measurements were also made below the top of the fuel. The results for the two single-zone cores are plotted in Figure 7.

Calculations of moderator worth have been performed using the diffusion theory code HFN with slab geometry. The four-group lattice constants were the same as for the radial calculations. For water heights below the top of the fuel the effect of dry (unmoderated) fuel above the homogenized core was neglected. Calculated values of moderator worth are 20-25% greater than measured values.

XII. TEMPERATURE COEFFICIENT

The temperature coefficient of reactivity was measured in the two single-zone cores over the temperature range between $\sim$ 20°C and $\sim$ 50°C. The moderator was heated (or cooled) in a storage tank and was pumped in and out of the reactor vessel between measurements.

Calculations of multiplication at several temperatures were performed using temperature-dependent lattice constants for both core and reflector, taking into account also the change in transverse leakage with temperature. One other effect that needs to be included in the calculation is the expansion of the lucite lattice plates. New lattice constants were calculated, taking into account the increase in lattice pitch with temperature. Multiplications were then calculated using these new lattice

constants and a temperature-dependent core radius. Measured and calculated temperature coefficients are compared in Figure 8.

XIII. KINETICS

The ratio of effective delayed-neutron fraction to mean neutron lifetime (β/ℓ) was obtained in the two single-zone cores from measurements of reactor noise. To find the frequency dependence of reactor noise, a magnetic tape recording of the noise was analyzed using a multi-channel frequency analyzer. Program LEARN[18] was used to fit an equation of the form

$$y = A_1 + \frac{A_2}{\omega^2}\left[\frac{\omega^2 + A_3}{\omega^2 + A_4}\right] \qquad (6)$$

to the data points. In Equation (6) y is the power per unit bandwidth and ω is 2π times the frequency; A_1 is a constant background noise contribution, A_2 is a parameter which characterizes the magnitude of the plateau, A_3 is a parameter which characterizes the low frequency break point, and A_4 is $(\beta/\ell)^2$.

The parameters for the functions which best fit the experimental points are listed in Table VII. Also listed in Table VII are values of β, ℓ, and β/ℓ which were calculated[19] using the transport theory code Program S.[20] A plot of experimental points and the corresponding fitted function are shown in Figure 9.

The scatter in the data points is considerable, which is reflected in the rather large standard deviations in the measured values of β/ℓ. The

measured values do not contain a correction for differences in frequency response of the filters. It is expected that a re-analysis, which includes such corrections, will lead to reduced errors in the fitted parameters.

The calculated kinetics parameters that are shown in Table VII were used to convert measured periods into units of reactivity. The calculated β_{eff} values were used to relate cents to % $\Delta k/k$.

TABLE I

NEUTRON ENERGY-GROUP BOUNDARIES

Group	Upper Energy	Lower Energy
1	10 MeV	11.7 keV
2	11.7 keV	2.38 eV
3	2.38 eV	0.683 eV
4	0.683 eV	0

TABLE II

SUMMARY OF CRITICAL LOADINGS FOR UO_2- 2 wt.% PuO_2 LATTICES[a]

Type of Fuel	Actual Critical # F.E.	Effect of 8% Fuel Followers	Effect of Lucite Templates	Effect of Lucite Sheets	Effect of Lucite Sleeves	Refined Critical # F.E.	Calculated k_{eff}
1	252.0	None	-0.8 ± 0.4	+0.6 ± 0.1	-0.2 ± 0.1	251.6 ± 0.4	0.989
1-3	290.0	+5.0 ± 1	-1.5 ± 1.0	+1.8 ± 0.2	-0.3 ± 0.15	295.0 ± 1.5	0.991
3	386.7	+7.6 ± 0.4	-1.6 ± 0.3	+1.1 ± 0.1	-0.3 ± 0.1	393.5 ± 0.5	0.991
3-2	353.35	+5.0 ± 0.4	-3.3 ± 1.0	+0.9 ± 0.2	-0.3 ± 0.1	355.7 ± 1.1	0.990
2-3	345.31	+5.1 ± 0.4	-3.5 ± 1.0	+0.55 ± 0.15	-0.3 ± 0.1	347.2 ± 1.1	0.990
3-1	318.8	+1.6 ± 0.1	-1.2 ± 0.6	+0.49 ± 0.08	-0.3 ± 0.1	319.4 ± 0.6	0.990
1[b]	252.16	None	-0.8 ± 0.4	+0.19 ± 0.05	-0.2 ± 0.1	251.4 ± 0.4	0.989

(a) All quantities are in terms of number of fuel elements.

(b) The 7.65% ^{240}Pu loading was repeated.

TABLE III

MEASURED AND CALCULATED BUCKLINGS AND REFLECTOR SAVINGS

Fuel Type	Critical Radius (cm)		Radial Reflector Savings (cm)		Axial Reflector Savings (cm)		B_r^2 (m^{-2})		B_{axial}^2 (m^{-2})	
	Exp.	Calc.	Exp.	Calc.	Exp.	Calc.	Exp.	Calc.	Exp.	Calc.
1	17.975	18.532	8.55 ± 0.53	6.70	6.96 ± 0.25	6.87	82.2 ± 3.3	90.86	8.89 ± 0.09	8.97
3	22.485	23.184	7.75 ± 0.33	6.85	6.32 ± 0.20	7.02	63.3 ± 1.4	64.14	9.11 ± 0.07	8.87
3-1	-	-	-	-	6.96 ± 0.28	-	-	-	8.89 ± 0.10	-
2-3	-	-	-	-	6.38 ± 0.30	-	-	-	9.09 ± 0.11	-
3-2	-	-	-	-	6.79 ± 0.36	-	-	-	8.95 ± 0.12	-

TABLE IV

COMPARISON BETWEEN SUBCRITICAL AND FLUX-SHAPE METHODS

	Subcritical Method			Critical Flux-Shape Method			
Fuel	λ^* cm	$B^2(M^{-2})^*$	N_c^*	λ_{radial}, cm	λ_{axial}, cm	B^2 (m^{-2})	Critical N_c
1	8.0	96.6 ± 1.5	244 ± 4	8.55 ± 0.53	6.96 ± 0.25	91.1 ± 3.3	251.5 ± 0.2
3	8.0	71.3 ± 0.8	380 ± 3	7.75 ± 0.33	6.32 ± 0.20	72.4 ± 1.4	393.5 ± 0.5

*Interpolated between results presented in Reference 3.
The RMS errors in B^2 and N_c were estimated on the basis of fitting[16] an analytical function to experimental data at other lattice pitches.

TABLE V

CALCULATED AND MEASURED FUEL ROD WORTH, CENTS

(For a Fuel Rod Replacing Water)

Fuel Type	Central Fuel Rod		Peripheral Fuel Rod	
	Exp.	Calc.	Exp.	Calc.
1	-23.2 ± 0.2	-34.8	21.0*	22.0
3	-15.3 ± 0.2	-23.0	10.2*	10.2

*Read off curves in Figure 5, at effective radius of core. The estimated uncertainty is ± 5%.

TABLE VI

CALCULATED AND MEASURED VOID WORTH

Fuel Type	Worth of 14% Void in Central Cell, Cents		14% Void Worth Integrated Over Core, $		Average Void Coefficient, ¢/% void	
	Exp.	Calc.	Exp.*	Calc.	Exp.*	Calc.
1	-12.8 ± 0.2	-9.9	-12.2	-15.7	-87	-112
3	- 7.5 ± 0.2	-5.4	- 9.9	-12.9	-71	- 92

*These experimental values do not include interaction effects between cells; the estimated uncertainty is ± 10%.

TABLE VII

PARAMETERS FOR EQUATION (6)
AND CALCULATED KINETICS PARAMETERS

Fuel Type	Parameters From Best Fit				
	A_1	A_2	A_3	A_4	β/ℓ
1	0.0	2.79×10^{5}	7.33×10^{-1}	1.624×10^{4}	127 ± 11
3	3.75×10^{4}	2.78×10^{5}	5.27×10^{-1}	1.302×10^{4}	114 ± 15

Fuel Type	Calculated Parameters		
	β	ℓ	β/ℓ, sec^{-1}
1	3.447×10^{-3}	3.064×10^{-5}	112.5
3	3.732×10^{-3}	2.944×10^{-5}	126.8

REFERENCES

1. R. A. Bennett and L. C. Schmid, "Approach-to-Critical and Calibration Experiments in the Plutonium Recycle Critical Facility," HW-80206, Hanford Works (July, 1964).

2. V. O. Uotinen, "Measurements of the Reactivity Worth of Hafnium-Oxide Rods in a PuO_2-UO_2-H_2O Lattice," *Trans. Am. Nucl. Soc.* 9, 2, 520 (Nov. 1966).

3. R. C. Liikala and W. P. Stinson, "Experimental and Analytical Results for PuO_2-UO_2-H_2O Lattices," *Trans. Am. Nucl. Soc.*, 9, 1, 126 (June 1966).

4. L. C. Schmid, et al, "Critical Masses and Bucklings of PuO_2-UO_2-H_2O Systems," *Trans. Am. Nucl. Soc.* 7, 2, 216 (1964).

5. F. G. Dawson, et al, "Analysis of Plutonium-Fueled Light Water Reactors," IAEA Symposium on the Use of Plutonium as a Reactor Fuel, Brussels, Belgium, March 13-17, 1967.

6. J. L. Carter, Jr., "Effective Cross Sections for Resonances in HRG," and "Computer Code Abstracts," *Technical Activities Quarterly Report, July, August, September, 1966*, USAEC Report BNWL-340, October 15, 1966.

7. H. C. Honeck, "THERMOS - A Thermalization Transport Theory Code for Reactor Lattice Calculations," BNL-5826, Brookhaven National Laboratory, and J. R. Worden, W. L. Purcell, and R. C. Liikala, "Modifications to the Computer Code THERMOS, and Comparative Studies on Scattering Kernels," *Physics Research Quarterly Report, July, August, September, 1965*, BNWL-193, pp. 5-15. October 15, 1965.

8. R. H. Shudde and J. Dyer, NAA Program Description, "Tempest - A Neutron Thermalization Code," North American Aviation Corporation, (1960).

9. J. R. Lilley, "Computer Code HFN-Multigroup, Multiregion Neutron Diffusion Theory in One Space Dimension," USAEC Report HW-71545, November, 1961.

10. M. Nelkin, "The Scattering of Slow Neutrons by Water," *Phys. Rev., Vol 19,* p. 791. (1960).

11. H. C. Honeck, "The Calculation of Thermal Utilization and Disadvantage Factor in Uranium/Water Lattices," *Nucl. Sci. Eng., Vol. 18, p. 49, 1964.*

12. ANL-5800, Second Edition, pp. 283-291.

13. K. B. Stewart, "BNW Master Library," Vols. I, II, III, BNWL-CC-325 (September 1, 1965).

14. C. H. Westcott, et al, "A Survey of Values of the 2200 m/x Constants for Four Fissile Nuclides," *Atomic Energy Review, 3, 2 (1965).*

15. P. F. Gast, "Light Water Lattices," IAEA STI/DOC/10/12, Vienna, 1962.

16. W. P. Stinson, Battelle-Northwest, Personal Communication (1967).

17. R. L. Hellens and E. Anderson, Brookhaven National Laboratory, BNL-7293, and H. H. Windsor, *Trans. Am. Nucl. Soc., 8, 1, 264* (June 1964).

18. B. H. Duane, "Maximum Likelihood Nonlinear Correlated Fields (Battelle Northwest Program LIKELY)," BNWL-390. September 15, 1965.

19. L. J. Page and V. O. Uotinen, Unpublished Data, BNW (1966).

20. B. H. Duane, "Neutron and Photon Transport, Plane-Cylinder- Sphere, GE-ANPD Program S, Variational Optimum Formulation," XDC 59-9-118 General Electric Aircraft Nuclear Propulsion Department. 1959.

ACKNOWLEDGEMENT

The authors thank Dr. Setsuo Kobayashi for analysis of the temperature coefficient experiment, and for many useful discussions concerning the analysis of other experiments. Dr. Kobayashi is a visiting physicist from the Central Research Laboratory of Hitachi, Ltd., Tokyo, Japan. The authors also thank J. H. Lauby for obtaining and analyzing the magnetic tape recordings of reactor noise.

#16 URE

Copper Activation Distribution

7.55% Pu^{240}

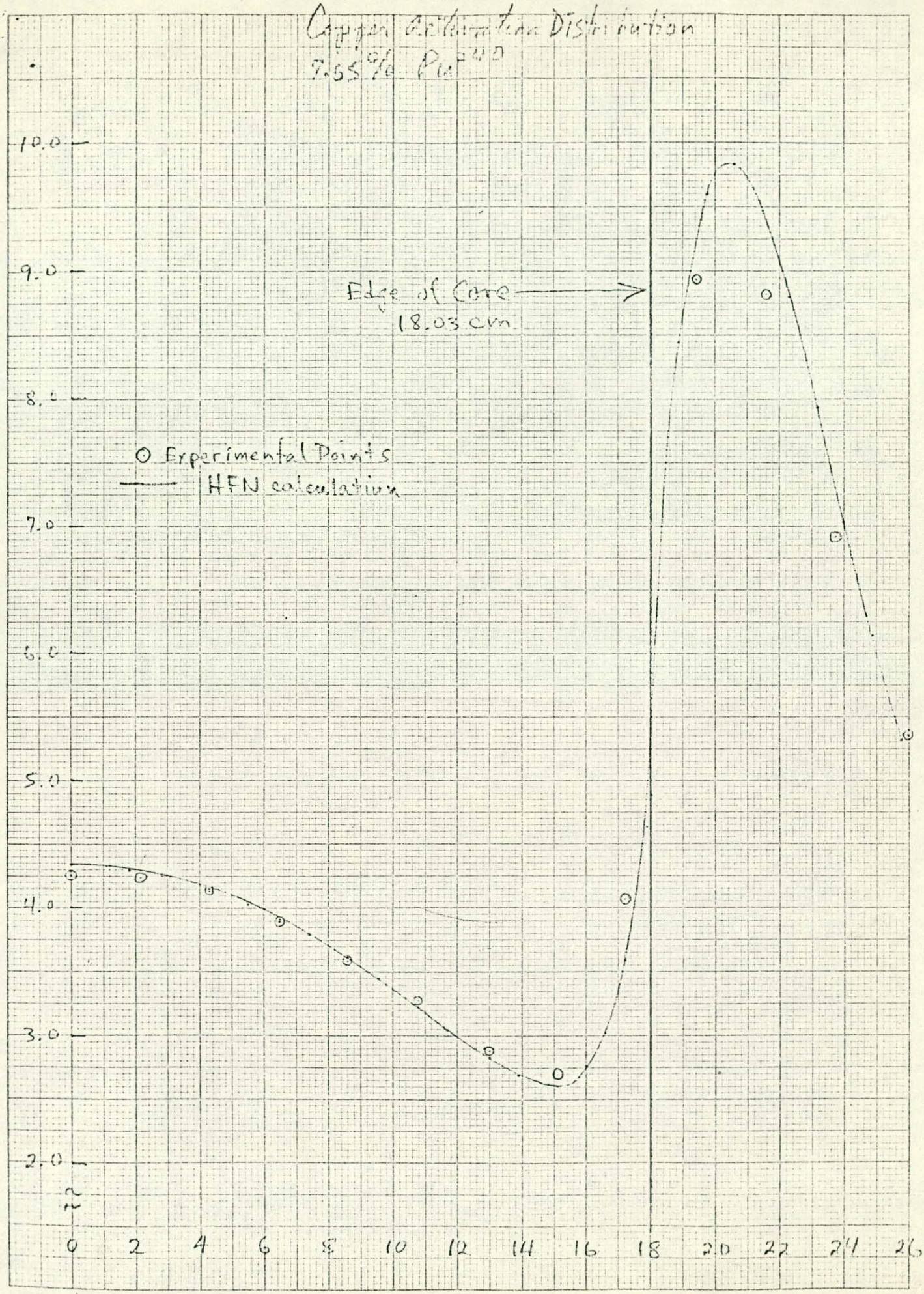

FIGURE 2

Copyright declassified Distribution
Bare Homo-Zoned Core
Inner Zone 23.5% Pu^{240}, Outer Zone 7.65% Pu^{240}

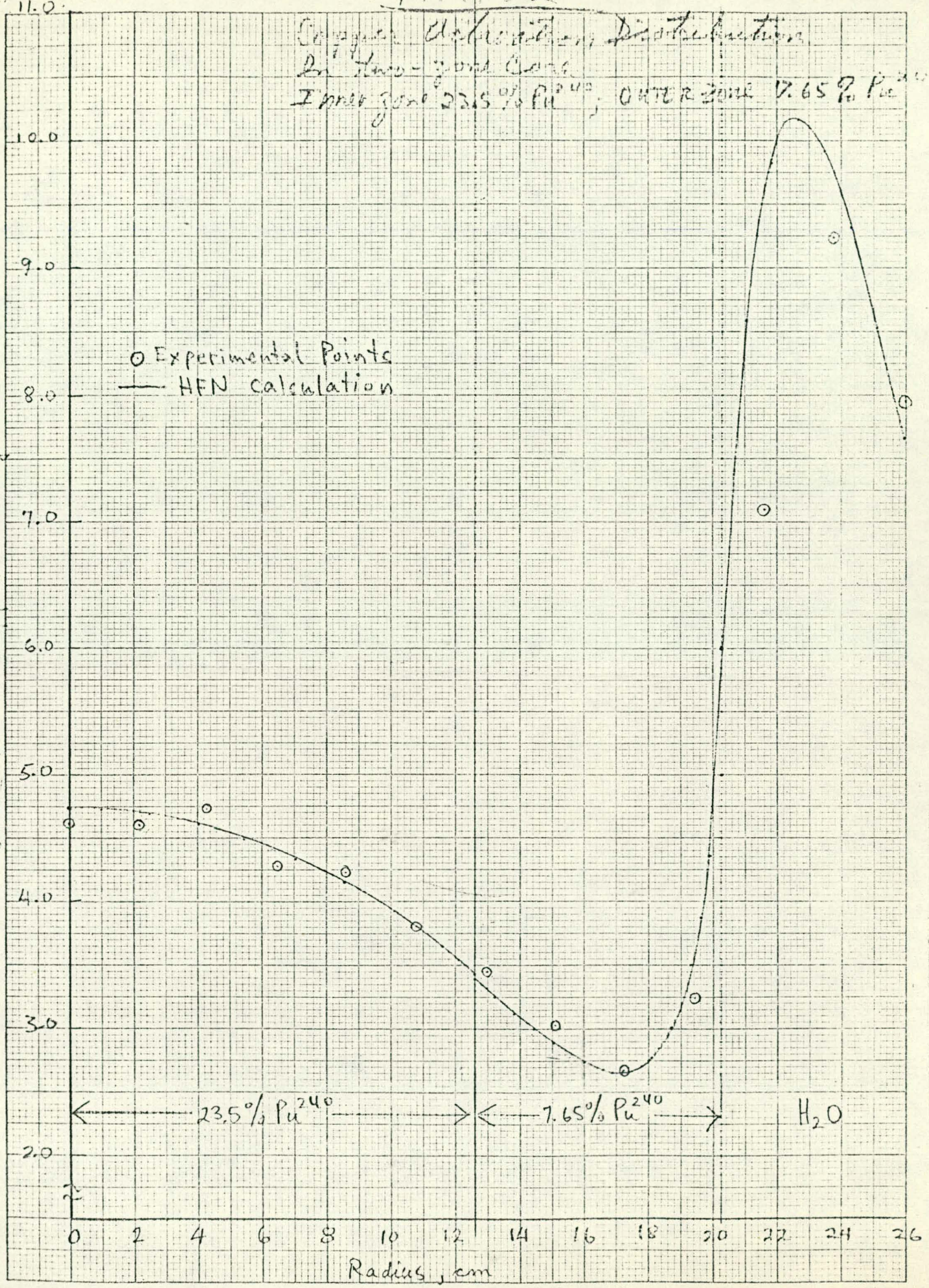

7.65 % Pu^{240}

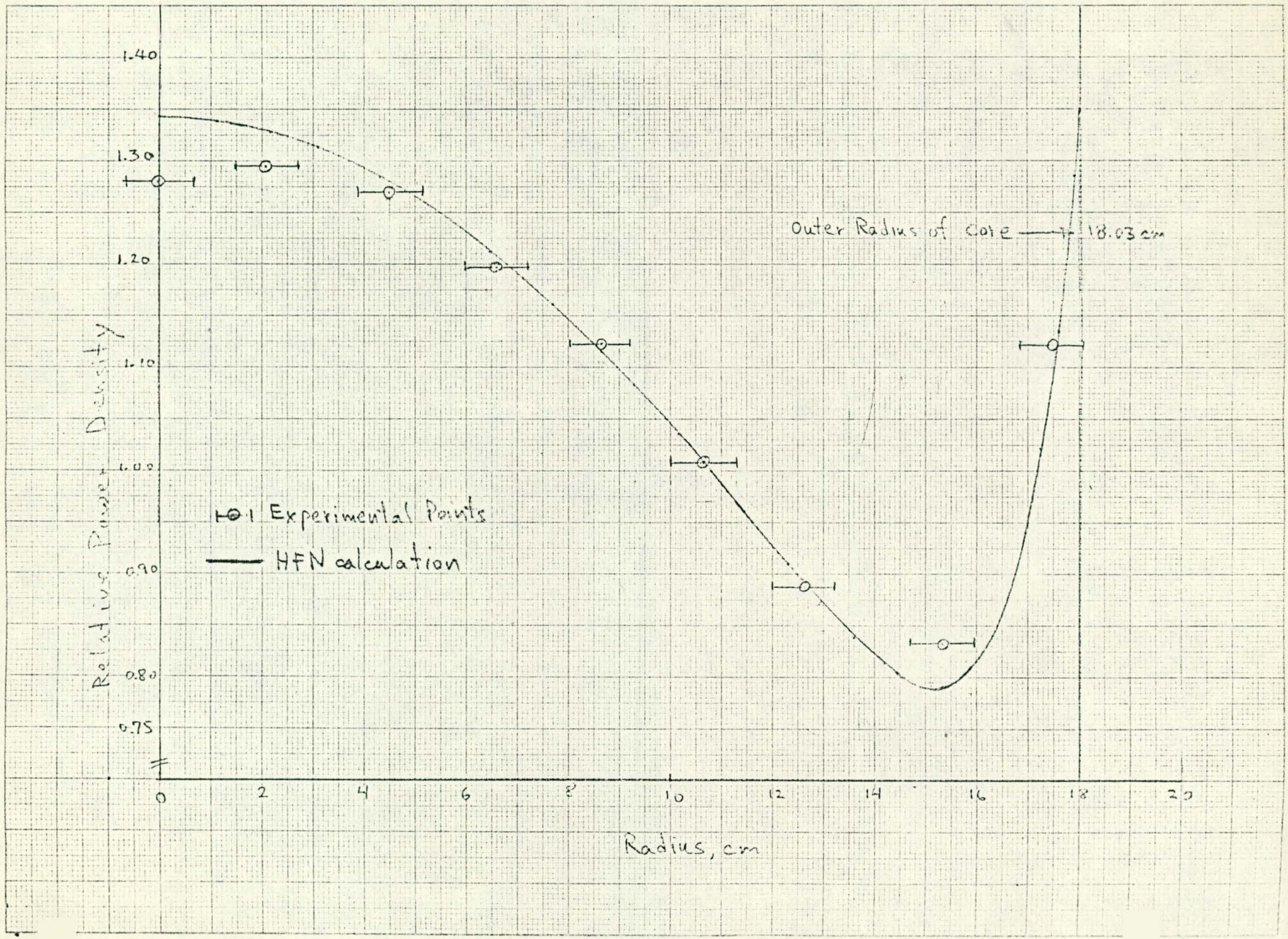

FIGURE 4

Power Density Distribution in Two-Zone Core.

INNER ZONE 16.54% Pu^{240}; outer zone 23.50% Pu^{240}

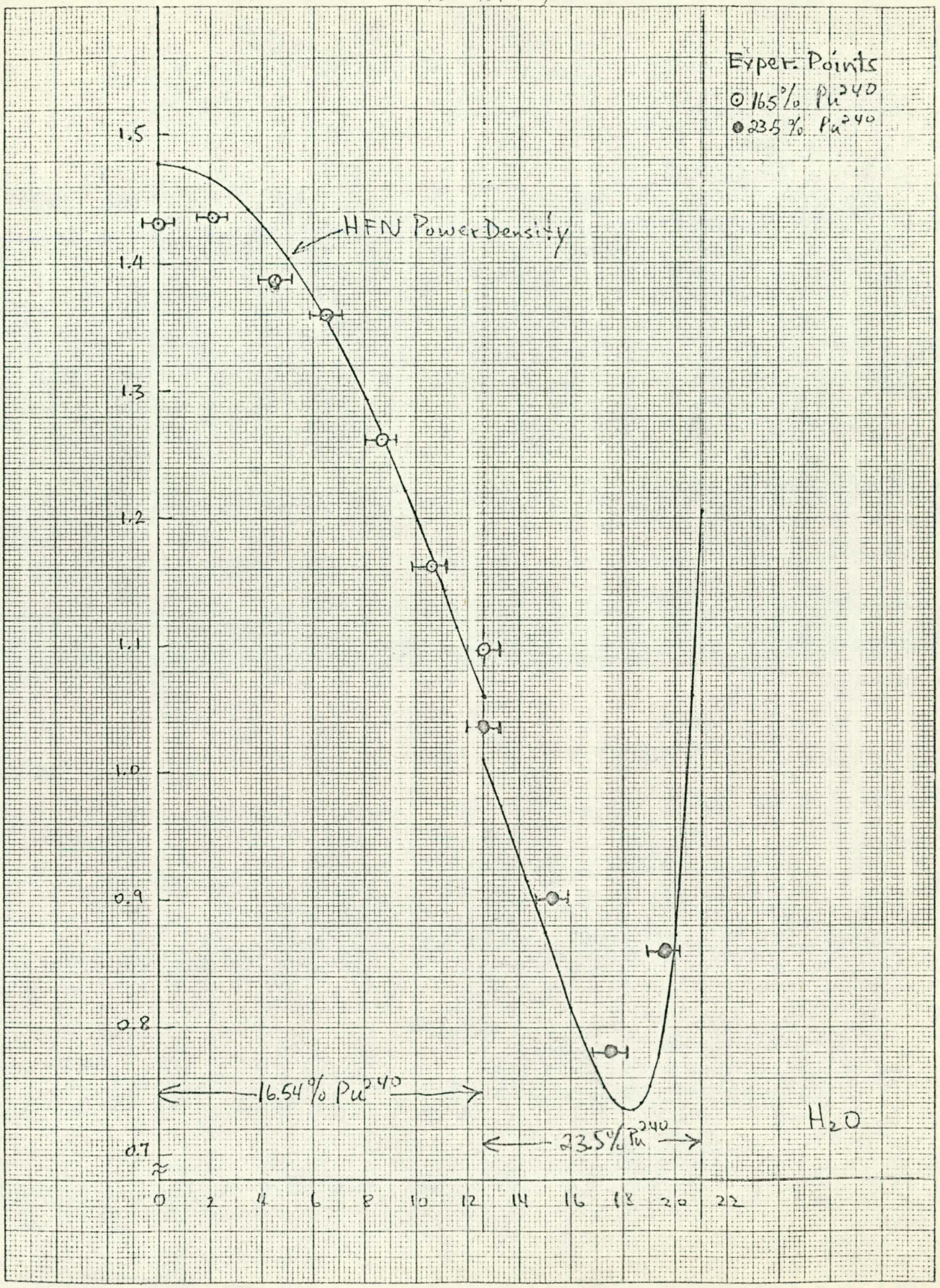

16% IN, 24% OUT

Figure 5

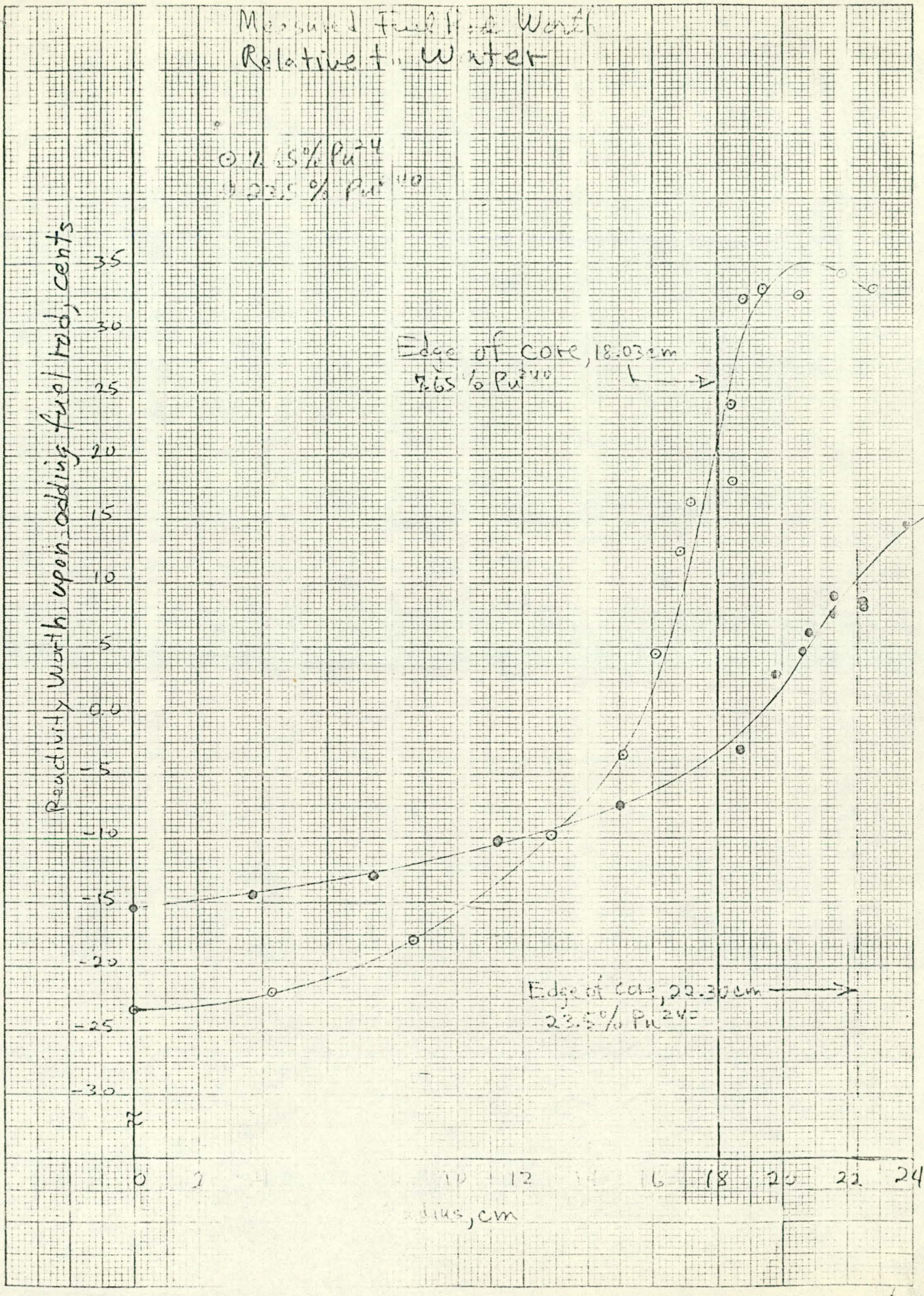

FIGURE 6

MEASURED VOID WORTH

RELATIVE TO WATER

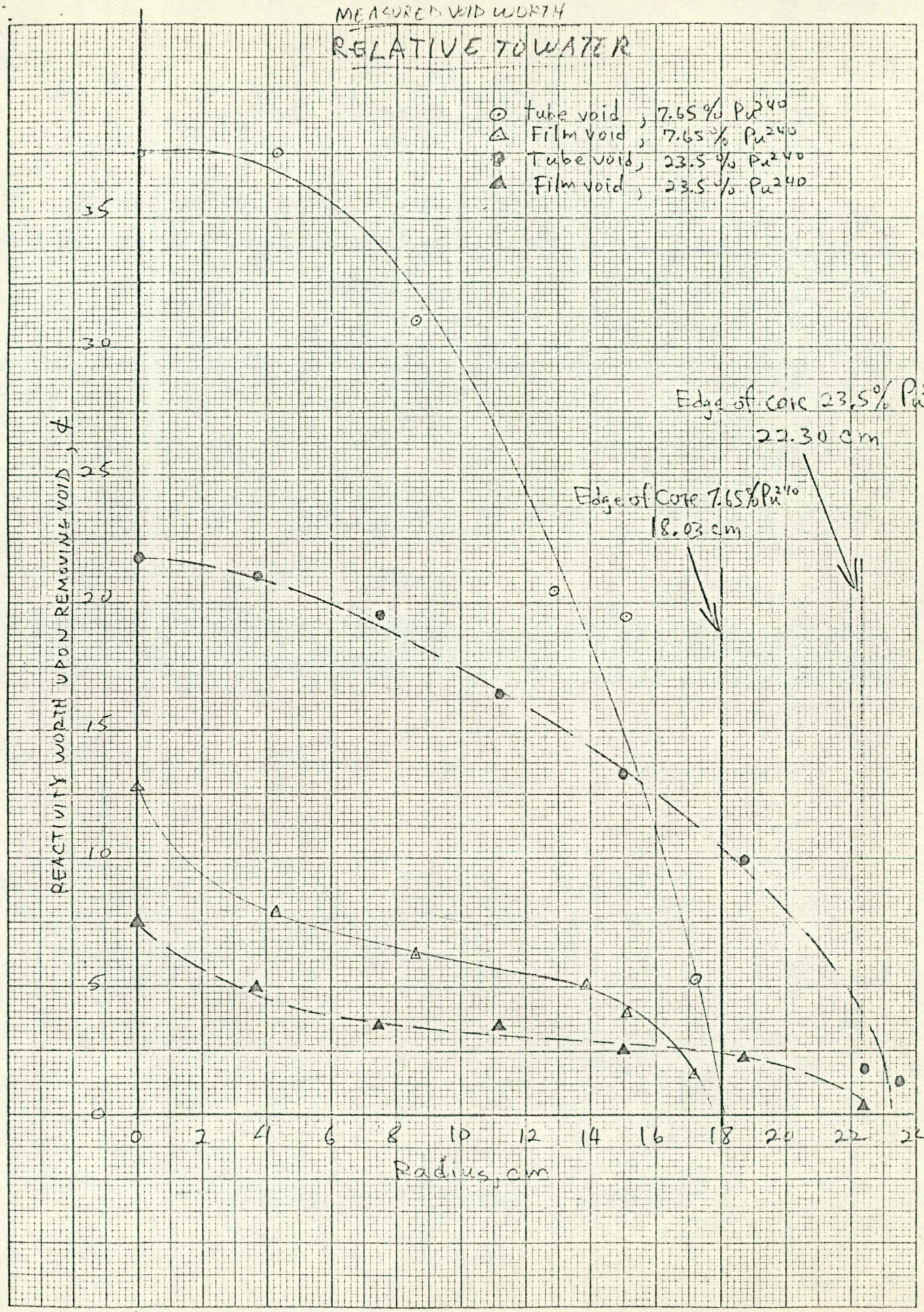

Figure 4 — Measured Effects of Moderator Height Changes.

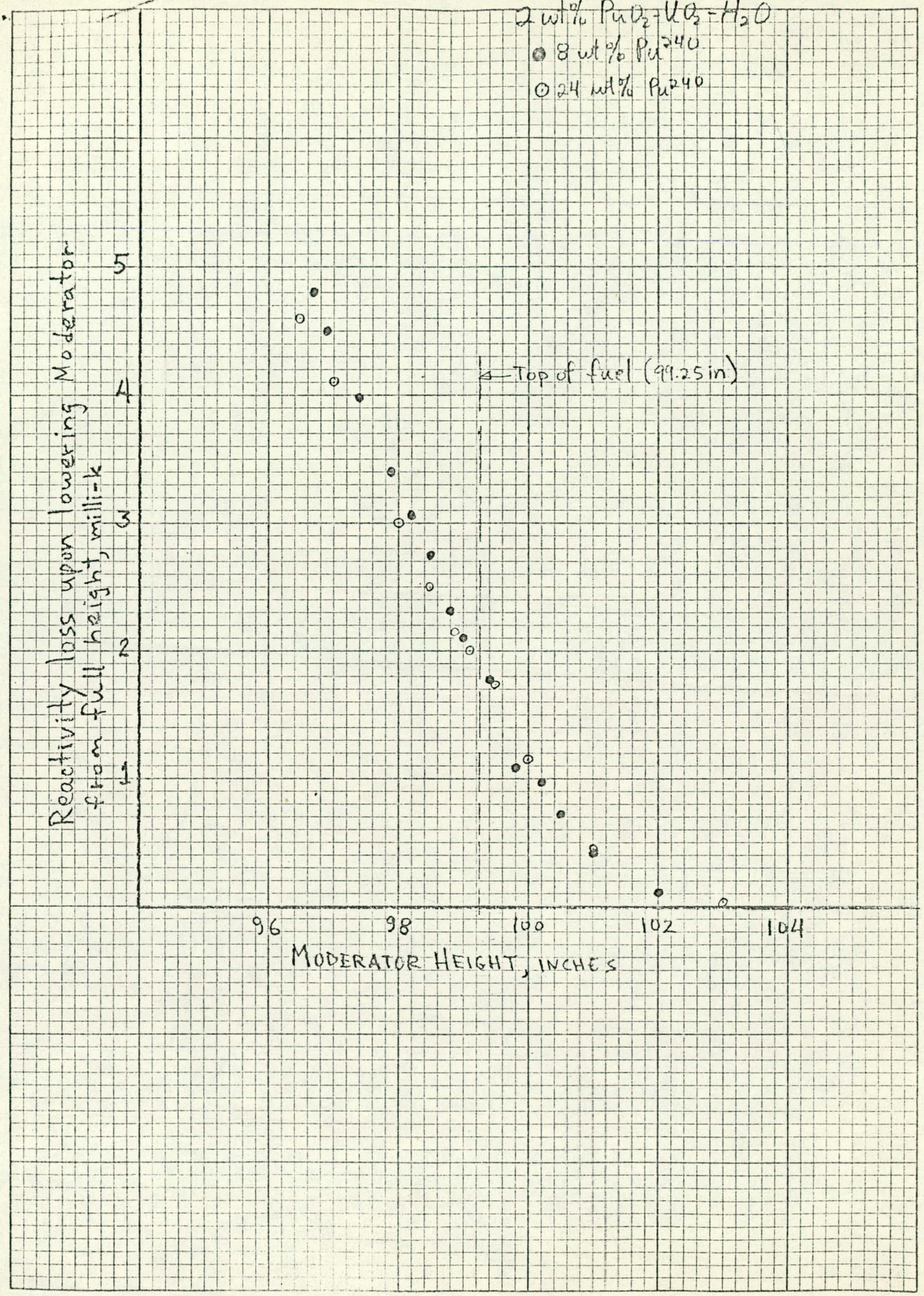

FIGURE 8 (Preliminary)

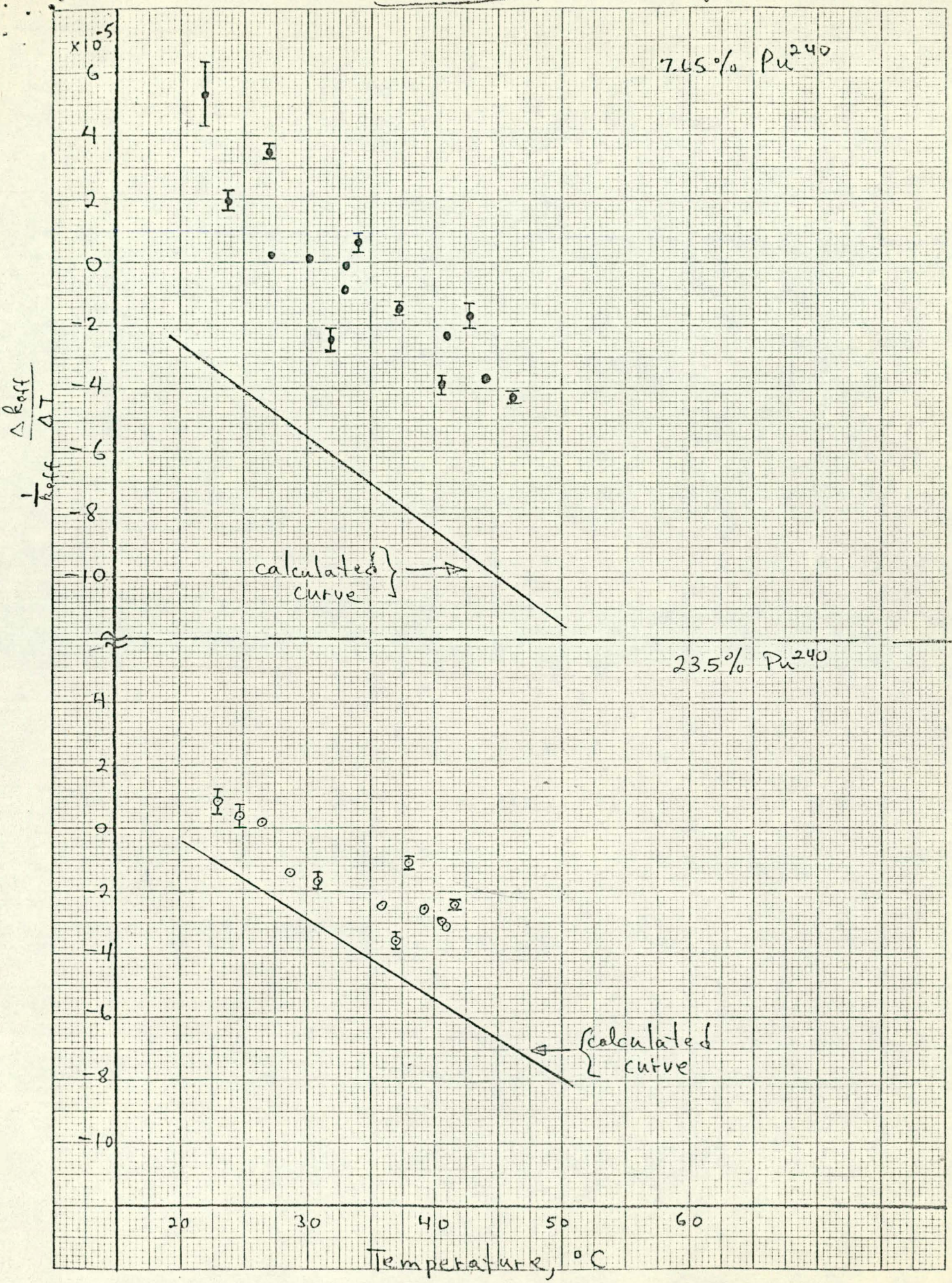

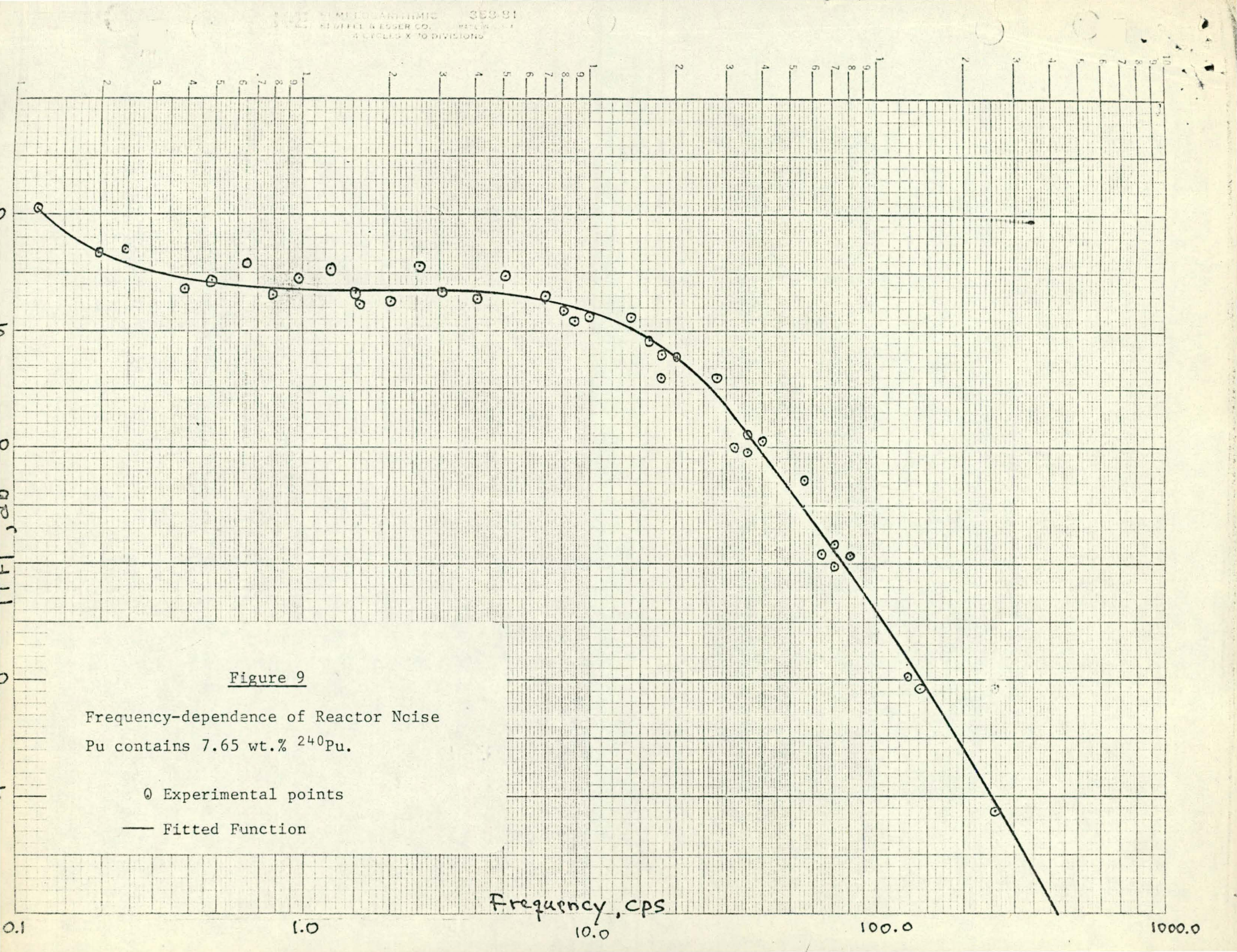

Figure 9

Frequency-dependence of Reactor Noise

Pu contains 7.65 wt.% ^{240}Pu.

0 Experimental points

—— Fitted Function